ACS APPLIED MATERIALS & INTERFACES

Research Article

Cite This: ACS Appl. Mater. Interfaces 2019, 11, 46671−46677

www.acsami.org

ZIF-8-Based Quasi-Solid-State Electrolyte for Lithium Batteries

Cui Sun,[†,§] Jin-hua Zhang,[†,§] Xiang-fei Yuan,[†] Jia-ning Duan,[†] Sheng-wen Deng,[†] Jing-min Fan,[†] Jeng-Kuei Chang,[‡] Ming-sen Zheng,*[,†] and Quan-feng Dong*[,†]

[†]State Key Laboratory for Physical Chemistry of Solid Surfaces, Department of Chemistry, College of Chemistry and Chemical Engineering, iChEM (Collaborative Innovation Center of Chemistry for Energy Materials), Xiamen University, Xiamen 361005, China

[‡]Department of Materials Science and Engineering, National Chiao Tung University, Hsinchu 30010, Taiwan

Supporting Information

ABSTRACT: The quasi-solid-state electrolytes (QSSEs) with an inorganic skeleton, a solid−liquid composite material combining their respective merits, exhibit high ionic conductivity and mechanical strength. However, most quasi-solid electrolytes prepared by immobilizing ionic liquid (IL) or organic liquid electrolyte in inorganic scaffold generally have poor interface compatibility and low lithium ion migration number, which limits its application. Herein, we design and prepare a ZIF-8-based QSSE (ZIF-8 QSSE) in which the ZIF-8 has a special cage structure and interaction with the guest electrolyte to form a composite electrolyte with good ionic conductivity about 1.05×10^{-4} S cm^{-1} and a higher lithium-ion transference number of about 0.52. With the ZIF-8 QSSE, a protype lithium battery coupled with $LiCoO_2$ cathode shows good electrochemical performances with an initial discharge capacity of 135 mAh g^{-1} at 50 mA g^{-1} and a remaining capacity of 119 mAh g^{-1} after 100 cycles, only 0.119% capacity degradation per cycle. It is worth noting that the ZIF-8-based QSSEs have good thermal stability up to 350 °C that does not show thermal runaway, which is significantly higher than that of a conventional organic liquid battery system.

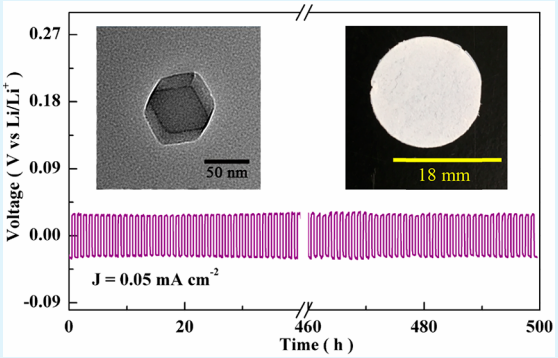

KEYWORDS: *ZIF-8, quasi-solid electrolyte, lithium-ion migration number, thermal stability, electrochemical performances, lithium batteries*

INTRODUCTION

Lithium-ion batteries (LIBs) with long cycle life and high energy density have attracted much attention as a promising alternative to conventional energy storage systems.[1−4] Due to the high flammability, liquid leakage of conventional batteries, solid-state electrolytes and/or quasi-solid-state electrolytes (QSSEs) have been regarded as promising candidate to improve the safety of the LIB battery systems.[5−8] Nowadays, QSSE with inorganic skeleton is usually prepared by immobilizing ionic liquid (IL) or organic liquid electrolyte in inorganic scaffold. In fact, they are a solid−liquid composite material combining their respective merits and exhibiting high ionic conductivity and mechanical strength which can suppress the lithium dendrite growth.

Metal−organic frameworks (MOFs) are a group of materials synthesized by assembling metal ions with organic ligands that have high surface area, abundant micropores, excellent thermal and chemical stability.[9−12] In addition to the common properties of gas adsorption[13] and separation,[14] their ion conductivity properties[15] has also been displayed. Furthermore, due to the pore size and interaction with guest molecules, MOFs can control the dynamics of small molecules and alter the interaction between MOFs and small molecules.[16] Recently, MOF[17−23] particles with open channels and stable frameworks are used as a carrier for a QSSE. However, the application of such QSSEs were limited due to the interfacial problem.[24] Therefore, it is essential to develop an optimized contact interface.

Directly dropping ILs onto the surface of a MOF membrane to achieve a good contact interface has been demonstrated, but there is limited interacting force between IL and MOF membrane.[24−27] As a MOFs series, ZIF-8 has been reported to be capable of controlling the kinetics of small molecules by nanosizing small molecules, and their ion transport path can be enhanced through increasing the concentration of guest ions.[18] Toward this end, we hypothesized the ZIF-8 with a special cage not only interacts with small solvent molecules but also ensures that lithium ions have continuous transport channels and good interface contact with electrode.

Here, we synthesized a ZIF-8 material with particle size about 50 nm via copolymerization method and prepared a ZIF-8 inorganic scaffold matrix film through a rolling method. By repeatedly impregnating normal organic liquid electrolyte and drying it in argon atmosphere, the organic liquid electrolyte

Received: August 7, 2019
Accepted: November 18, 2019
Published: November 18, 2019

DOI: 10.1021/acsami.9b13712
ACS Appl. Mater. Interfaces 2019, 11, 46671−46677

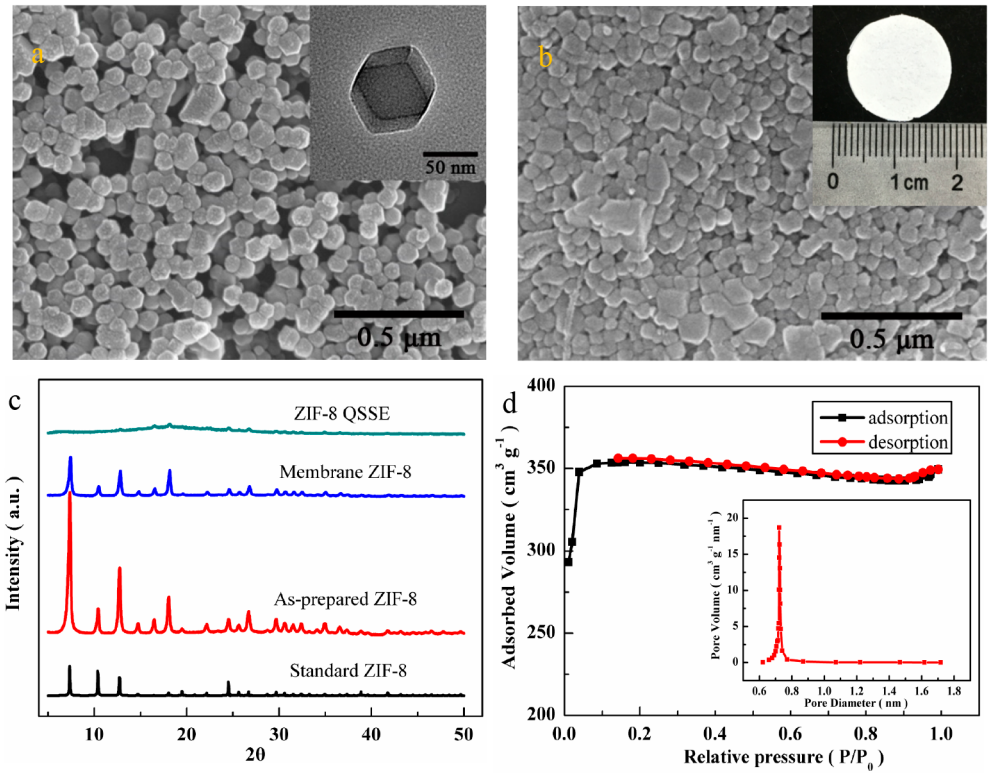

Figure 1. (a) SEM image showing the morphology of as-prepared ZIF-8 (inset: the corresponding TEM image of ZIF-8). (b) SEM image of the ZIF-8 membrane (inset: the photograph of ZIF-8 membrane). (c) Powder X-ray diffraction patterns of simulated ZIF-8, as-prepared ZIF-8, ZIF-8 membrane and ZIF-8 QSSE. (d) Ar adsorption−desorption analysis of the ZIF-8 membrane.

could be fixed in the ZIF-8 inorganic scaffold matrix film with both good ionic conductivity (10^{-4} S cm^{-1}) and high lithium-ion transference number (0.52). With the ZIF-8 QSSE, a $LiCoO_2$-based battery shows good electrochemical performances with an initial discharge capacity of 135 mAh g^{-1} at 50 mA g^{-1} and a remaining capacity of 119 mAh g^{-1} after 100 cycles.

EXPERIMENTAL SECTION

Synthesis of ZIF-8 Nanoparticles. All chemicals were purchased and used directly without further treatment. The ZIF-8 was obtained by one-step copolymerization of Zn(II) with 2-methylimidazolelinks. Typically, 5 mmol of zinc nitrate hexahydrate ($Zn(NO_3)_2{\cdot}6H_2O$) and 20 mmol of 1,2-dimethylimidazole were dissolved in 100 mL methyl alcohol. The copolymerization reaction was performed at room temperature without any interruption for 24 h after stirring for 2 min. The resulting white precipitate was centrifuged and washed three times with methanol before drying in vacuum glove box at 60 °C overnight.

Synthesis of the ZIF-8-Based QSSE. The ZIF-8 membrane was prepared by mixing 85 wt % ZIF-8 nanoparticles with 15 wt % polytetrafluoroethylene (PTFE), filming by a rolling method and drying in vacuum glove box at 120 °C for 24 h. Then, the ZIF-8 membrane was impregnated by organic liquid electrolyte (1 M $LiPF_6$ EC/DMC/EMC = 1:1:1) for 5 min, argon-dried for 5 min, and the above procedure repeated 4 times. The preparation of ZIF-8-based QSSE (ZIF-8 QSSE) must be carried out in the full argon gas vacuum glove box (water and oxygen content need below 0.01 ppm).

Synthesis of the TiO_2-Based QSSE. The same procedure as that for ZIF-8-based QSSE was used. Briefly, PTFE and TiO_2 (99.8%, 10−25 nm, Aladdin) were mixed at a ratio of 8:2 to form a film. Repeated soaking and drying was carried out to obtain a TiO_2-based QSSE.

Material Characterization. The morphology of the as-prepared products was observed on a Hitachi S-4800 scanning electron microscope (SEM) with a field-emission electron gun. Transmission electron micros-copy (TEM) image was obtained from a TECNAI F30 at 300 kV. The structure was characterized by X-ray powder diffraction (XRD, Philips Panalytical X-pert). The argon adsorption and desorption isotherm was measured at 77 K with a Micromeritics ASAP 2020 surface area and pore analyzer. The ionic conductivity of the ZIF-8 QSSE were measured using an electrochemical impedance analyzer (IM6 Electrochemical Workstation, Germany) at various temperatures (25, 40, 55, and 70 °C) in the frequency range from 10 mHz to 100 kHz by sandwiching the ZIF-8 QSSE between two stainless-steel blocking electrodes. The Li plating/stripping cycles were conducted at a constant current density on a NEWARE battery testing system (Shenzhen NEWARE Co., China). The electrochemical window of ZIF-8 QSSE was measured by linear sweep voltammetry (LSV) test of CHI660 (Shanghai Chenhua instrument co. LTD) at the scan rate of 0.5 mV s^{-1} in a cell composed of SS |ZIF-8 QSSE| Li in the voltage range of 0−5.5 V at room temperatures. The lithium ion migration number was calculated using formula as proposed by Vincent and co-workers. The thermal stability of the ZIF-8 QSSE and organic liquid electrolyte were evaluated by an accelerating rate calorimeter (Accelerated Rate Calorimetry, North House, Bletchley, MK11SW, UK) in the temperature range of 80−350 °C under adiabatic condition. The content of confined organic liquid electrolyte in the ZIF-8 QSSE was evaluated by thermogravimetric analysis (TGA) carried out under N_2 atmosphere at a heating rate of 10 °C min^{-1}.

Electrochemical Measurement. The anode electrode was prepared by mixing 80 wt % lithium cobalt oxide ($LiCoO_2$), 10 wt % acetylene black, and 10 wt % LA binders. The obtained slurries were then coated onto Al foil current collectors and dried at 60 °C under vacuum overnight. The $LiCoO_2$, a metallic lithium, and the ZIF-8 QSSE were sealed into a CR2016-type coin cell. The cycle voltammetry (CV) was carried out using an IVIUM Multichannel Electrochemical Analyzer. The charge−discharge cycling and rate tests were carried out on a NEWARE BTS-5 V/5 mA type battery

DOI: 10.1021/acsami.9b13712
ACS Appl. Mater. Interfaces 2019, 11, 46671−46677

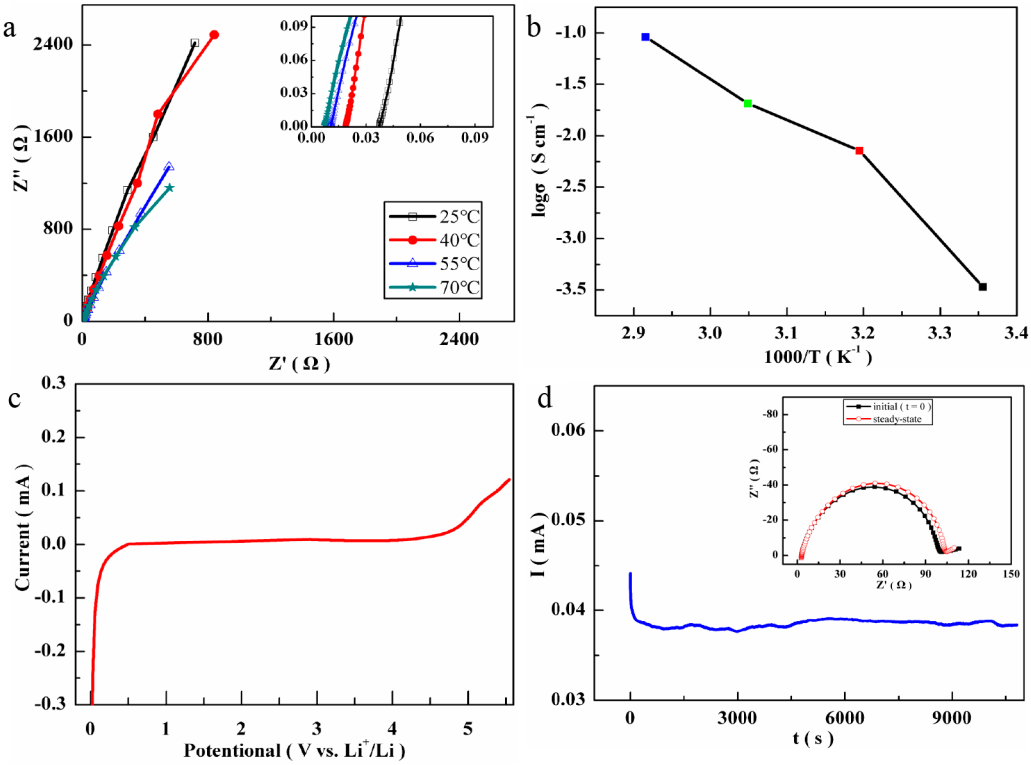

Figure 2. (a) Impedance spectra of the ZIF-8 QSSE at various temperature. (b) Ionic conductivity as a function of inverse temperature for the ZIF-8 QSSE. (c) Electrochemical window of ZIF-8 QSSE. (d) Chronoamperometric curve of SS |ZIF-8 QSSE| Li cell after a perturbation of 5 mV direct current (dc) pulse (inset: the corresponding impedance spectrum of the cell before and after the dc polarization at 25 °C, respectively).

charger (Shenzhen NEWARE Co, China) over the voltage range of 3.0−4.2 V at various temperatures.

RESULTS AND DISCUSSION

Material Characterizations. The as-prepared ZIF-8 and ZIF-8 membrane were characterized by scanning electron microscopy (SEM) and transmission electron microscopy (TEM). As shown in Figure 1a, the as-prepared ZIF-8 particles have a uniform particle size of less than 50 nm with a rhombic dodecahedral shape and the particles in ZIF-8 membrane still maintain the original morphology and similar size (Figure 1b). After impregnating the organic liquid electrolyte, the surface morphology of ZIF-8 QSSE has significant changes, as shown in Figure S1. There is no obvious gap on the surface of the ZIF-8 QSSE. This change may be caused by the combination of PTFE and ZIF-8 porous particles after infiltration.

The liquid retention rate of the ZIF-8 QSSE with time of drying in argon atmosphere are depicted in Figure S3. The liquid retention rate decreases in the first 10 min and remains very steady after 25 min of drying that indicates the good interaction between the liquid electrolyte and the ZIF-8 framework. The as-prepared ZIF-8 particles show high crystallinity without any detectable byproducts as revealed by the powder X-ray diffraction (XRD) pattern and the ZIF-8 membrane also mostly corresponded to the powder ZIF-8's characteristic peaks (Figure 1c). The XRD test results of the ZIF-8 QSSE showed no obvious crystallization peak, indicating that the lithium salt was dissociated in the ZIF-8 channel. To further investigate the porous structure of the ZIF-8 particles and the ZIF-8 membrane, Ar adsorption−desorption analysis was performed at 77 K. These measurements reveal that ZIF-8 particles and ZIF-8 membrane both belonged to a type I Langmuir isotherm. The ZIF-8 particles show a Brunauer−Emmett−Teller (BET) surface area of 1460 m^2 g^{-1} (Figure S2), while the ZIF-8 membrane shows a BET surface area of 1180 m^2 g^{-1} that retains the ZIF-8 micropore structures which are beneficial for confining electrolytes. The size of the micropores is about 0.7 nm, as derived by using the Horvath−Kawazoe method (Figure 1d). In a word, the ZIF-8 nanoparticles have a good film-forming property and liquid absorption properties, which is of great importance to display good ion conductivity.

The thermal stability of the electrolyte plays a vital role in determining the safety of lithium batteries. Once the temperatures reached more than 120 °C, corresponding to the boiling point of the nonaqueous liquid electrolyte solvents (DMC, EMC) and the melting point of the commercially available Celgard membrane, the battery with organic liquid electrolyte may cause a series of safety problems.[6] In order to investigate the thermal stability of the ZIF-8 QSSE, thermos-gravimetric studies had been conducted under a nitrogen flow and were shown in Figure S4. Clearly, ZIF-8 membrane is thermally stable up to 500 °C, and the ZIF-8 QSSE has a weight loss. The mass reduction rate is lower than organic liquid electrolyte in the same temperature range. During in 200−350 °C, ZIF-8 QSSE demonstrated slightly weight loss, indicating that the part solvents were it. The contents were estimated to be 48 wt % ZIF-8 and 45 wt % organic liquid electrolyte (Table S1).

The ionic conductivities of the ZIF-8 QSSE at various temperatures (25, 40, 55, and 70 °C) were depicted in Figure 2b. The detailed ionic conductivity test results and fitting data were shown in Figure 2a and Table S2. The ionic conductivity of ZIF-8 QSSE increase with rising temperature and its

DOI: 10.1021/acsami.9b13712
ACS Appl. Mater. Interfaces 2019, 11, 46671−46677

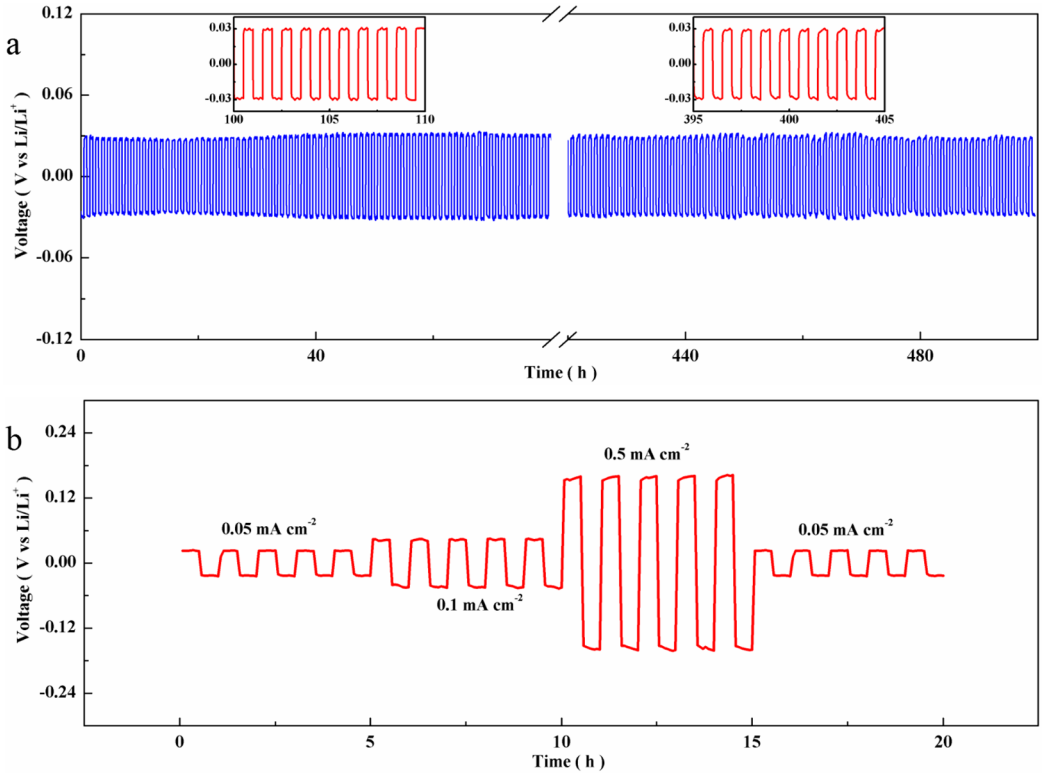

Figure 3. (a) Voltage profiles for the Li |ZIF-8 QSSE| Li symmetric cell at the current density of 0.05 mA cm^{-2} (inset: the corresponding voltage profiles of the cell at 95−305 cycles and at 395−405 cycles). (b) Voltage profiles for the Li |ZIF-8 QSSE| Li symmetric cell at current densities of 0.05, 0.1, and 0.5 mA cm^{-2}.

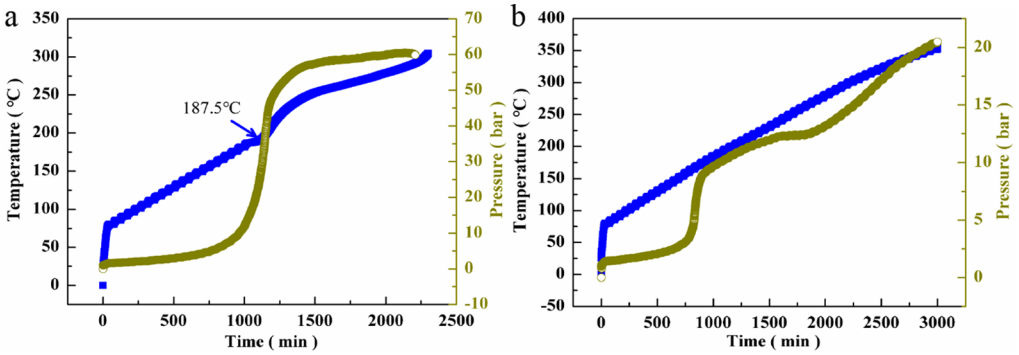

Figure 4. *T* and *P* vs time curves for the ARC of organic liquid electrolyte (a) and ZIF-8 QSSE (b).

behavior confirm to the Arrhenius equation. The ionic conductivity of ZIF-8 QSSE varies from 10^{-4} S cm^{-2} (25 °C) to 10^{-3} S cm^{-2} (70 °C). The activation energy calculated by the formula of Arrhenius formula is 0.458 eV. To compare the ZIF-based electrolyte and non-ZIF-based electrolyte, we prepared the TiO_2-based QSSE. The ionic conductivities of the ZIF-8 QSSE at various temperatures (25, 40, 55, and 70 °C) and the photograph were depicted in Figure S5. The surface of the QSSE prepared by TiO_2 is very smooth; the conductivity is on the order of 10^{-5} S cm^{-1} at room temperature, which is slightly lower than ZIF-8-based QSSE. The electrochemical window of the ZIF-8 QSSE is about 0∼4.7 V as shown in Figure 2c. When scanned to a higher potential, a sharp increase of current appears, indicating an oxidative degradation of the organic liquid electrolyte. These results illustrate that the ZIF-8 QSSE was stable for practical application in lithium-ion battery. Figure 2d shows the chronoamperometric curves of the ZIF-8 QSSE. The insets show the Nyquist plots before and after perturbation. Through the corresponding calculation, the lithium ion transference number of ZIF-8 QSSE is about 0.52.

The stability of Li plating/stripping processes was carried out by galvanostatic charge−discharge cycling at room temperature. Figure 3a shows the time-dependent voltage profile of the Li |ZIF-8 QSSE| Li symmetric lithium cell at the current density of 0.05 mA cm^{-2} for 500 cycles. As shown in Figure 3a, the voltage keeps stable at about 26 mV without obviously change for 500 cycles, which suggests a stable interface between the ZIF-8 QSSE and the Li metal during cycling. Figure 3b shows the time-dependent voltage profile of the symmetric lithium cell at different current densities, the voltage remains stable at 22, 44, and 160 mV at the current densities of 0.05, 0.1, and 0.5 mA cm^{-2}, respectively, which indicates that the ZIF-8 QSSE with Li metal still has stable interface even at larger currents. In comparison, the voltage

DOI: 10.1021/acsami.9b13712
ACS Appl. Mater. Interfaces 2019, 11, 46671−46677

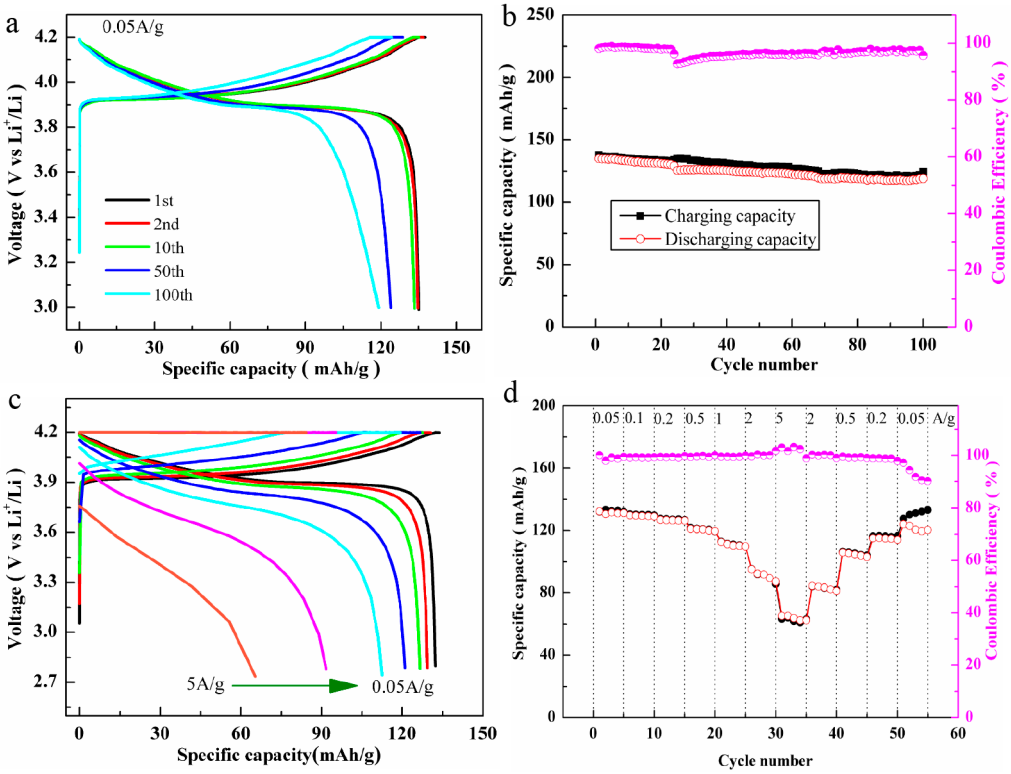

Figure 5. Electrochemical properties of the quasi-solid-state battery at 25 °C. (a) Voltage capacity profile of the quasi-solid-state lithium battery at 0.05 A g^{-1}. (b) Cycling performance and Coulombic efficiency of the quasi-solid-state lithium battery at 0.05 A g^{-1}. (c) Voltage capacity profiles of the quasi-solid-state lithium battery at increasing current densities from 0.05 to 5 A g^{-1}. (d) Rate capability of the quasi-solid-state lithium battery at increasing current densities from 0.05 to 5 A g^{-1}.

curves are very stable in ZIF-8 QSSE, but fluctuate greatly in organic liquid electrolyte (Figure S6), especially at a larger current density. Moreover, the ZIF-8 skeleton with a certain strength can suppress the growth of lithium dendrites, thereby further stabilizing the interface between electrolyte and the lithium metal.[28−31] A symmetric cell composed of Li |ZIF-8 QSSE| Li was assembled to further investigate the stability of the QSSE to lithium by the impedance spectra. The results were exhibited in Figure S7. The values of the resistance can be carried out by the Rb(RctQ)W circuit fitting and calculated from the Nyquist impedance plots. It is clearly that the resistance does not have an order of magnitude change even after 14 days, which indicates a good stability between the QSSE and lithium.

The flame resistance and safety are important aspects for electrolyte or separator in batteries. It is well-known that the commercial Celgard separator wetted by organic liquid electrolyte is easy to severely thermal shrink at 100 °C and completely burned at 200 °C. The inflammable Celgard separator could cause internal short-circuits and thus lead to fire outbreaks and even explosion. Figure 4a shows the temperature and pressure plot of organic liquid electrolyte in different organic liquid systems. The onset temperature is around 187.5 °C, approximately corresponding to the decomposition temperature of $LiPF_6$, which will easily result in thermal runaway for a lithium-ion battery.[6] The pressure increases rapidly with temperature rising and reaches its maximum and stable at 60 bar, which corresponds to the solvent decomposition. However, the ZIF-8 QSSE, as shown in Figure 4b, does not reach the onset temperature at the temperature range for several minutes, which indicates that the onset temperature of ZIF-8 QSSE is higher than 350 °C. The pressure increases rapidly with rising temperature that possibly corresponds to the solvent evaporation in ZIF-8 matrix, while it increases flatly and reaches its maximum at 20 bar. This indicates that the organic liquid electrolytes are fixed into the ZIF-8 micromatrix very well, resulting in a good composite electrolyte with improved flame resistance and safety properties.

Electrochemical Measurements. The CV curves of the quasi-solid-state lithium battery are similar to those of the conventional batteries with organic liquid electrolyte (Figure S8). The impedance parameters of the quasi-solid-state lithium battery are slightly higher than that of the liquid lithium battery but are still in the same magnitude, as is shown Figure S9.

To evaluate the electrochemical properties of the ZIF-8 QSSE, the quasi-solid-state battery had been tested by using a 2016-type coin cell. Figure 5a shows the corresponding discharging/charging voltage profiles of the quasi-solid-state battery at 0.05 A g^{-1} current density under room temperature. The discharging voltage profiles are characterized by a plateau (3.9 V) behavior of a typical $LiCoO_2$ cathode, while the charging voltage profiles exhibit a platform at around 3.95 V at 0.05 A g^{-1}. This is in good agreement with the reduction and oxidation peaks in the CV curves. The cycling performance of the quasi-solid-state lithium battery is shown in Figure 5b. At the current density of 0.05 A g^{-1}, the quasi-solid-state lithium battery could deliver a high initial reversible capacity of 135 mAh g^{-1} that is slightly lower than the normal liquid lithium battery (Figure S10), and the capacity still has 119 mAh g^{-1} after 100 cycles with a slow capacity decay rate of 0.119% per cycle, and Coulombic efficiency is almost 100%. As shown in

DOI: 10.1021/acsami.9b13712
ACS Appl. Mater. Interfaces 2019, 11, 46671−46677

Figure 5c,d, the quasi-solid-state cell exhibited excellent rate performance that is slightly better than that of the normal liquid lithium battery (Figure S11). At the current density of 0.05 A g^{-1}, it could deliver a discharge capacity of 135 mAh g^{-1}. When the current density was increased to 0.1 A g^{-1}, a specific capacity of 130 mAh g^{-1} was retained, which slowly reduced to 127 mAh g^{-1} at 0.2 A g^{-1}, 121 mAh g^{-1} at 0.5 A g^{-1}, 113 mAh g^{-1} at 1.0 A g^{-1}, 95 mAh g^{-1} at 2.0 A g^{-1}, 65 mAh g^{-1} at 5 A g^{-1}, and then finally recovered to 120 mAh g^{-1} at 0.05 A g^{-1} after 4 cycles. Furthermore, both the discharge and charge capacities are stable at different current densities, and the Coulombic efficiency was almost 100%. The quasi-solid-state batteries have superior cycle stability compared to organic liquid batteries, which is attributed to the formation of a relatively stable interface between the electrodes and the organic liquid electrolyte defined in the ZIF-8 frame. To further illustrate the excellent electrochemical performance of the quasi-solid-state battery, we conducted high temperature testing at 55 °C, which is shown in Figure S12. The quasi-solid-state battery has more excellent cycling performance at 0.05A g^{-1} current density, and it still has a capacity of 120 mAh/g after 60 cycles. However, in comparison to the room temperature, the polarization voltage changes largely with the high *C* rates.

CONCLUSIONS

In summary, we have developed a ZIF-8-based composite electrolyte with improved electrode interfaces and high battery safety. The ZIF-8-based QSSE exhibits high ionic conductivity (10^{-4} S cm^{-1} at 25 °C) and higher lithium-ion transference number (0.52). The ZIF-8-based QSSE demonstrated good thermal stability up to 350 °C. A $LiCoO_2$-based battery with the QSSEs exhibits excellent electrochemical performance that delivers a capacity of 135 mAh g^{-1} at 50 mA g^{-1} and maintains 119 mAh g^{-1} after 100 cycles with only 0.119% capacity degradation per cycle and even the current density is increased to 5 A g^{-1}, a specific capacity of 65 mAh g^{-1} can be retained.

ASSOCIATED CONTENT

Supporting Information

The Supporting Information is available free of charge at https://pubs.acs.org/doi/10.1021/acsami.9b13712.

Detailed descriptions of the BET, TG, CV, EIS, charging and discharging characterizations of ZIF-8 QSSE, and supplementary electrochemical data (PDF)

AUTHOR INFORMATION

Corresponding Authors

*E-mail: qfdong@xmu.edu.cn (Q.D.).
*E-mail: mszheng@xmu.edu.cn (M.Z.).

ORCID

Ming-sen Zheng: 0000-0001-9302-4631
Quan-feng Dong: 0000-0002-4886-3361

Author Contributions

§C.S. and J.H.Z. contributed equally to this work.

Notes

The authors declare no competing financial interest.

ACKNOWLEDGMENTS

We gratefully acknowledge the financial support from the National 973 Program (2015CB251102), the Key Project of National Natural Science Foundation of China (U1805254, 21673196, 21621091, 21703186), and the Fundamental Research Funds for the Central Universities (20720150042, 20720170101).

REFERENCES

(1) Tarascon, J. M.; Armand, M. Issues and challenges facing rechargeable lithium batteries. *Nature* **2001**, *414*, 359−367.
(2) Dunn, B.; Kamath, H.; Tarascon, J.-M. Electrical Energy Storage for the Grid: A Battery of Choices. *Science* **2011**, *334*, 928−935.
(3) Chu, S.; Majumdar, A. Opportunities and challenges for a sustainable energy future. *Nature* **2012**, *488*, 294−303.
(4) Thackeray, M. M.; Wolverton, C.; Isaacs, E. D. Electrical energy storage for transportation—approaching the limits of, and going beyond, lithium-ion batteries. *Energy Environ. Sci.* **2012**, *5*, 7854−7863.
(5) Xu, K. Nonaqueous Liquid Electrolytes for Lithium-Based Rechargeable Batteries. *Chem. Rev.* **2004**, *104*, 4303−4417.
(6) Kalhoff, J.; Eshetu, G. G.; Bresser, D.; Passerini, S. Safer Electrolytes for Lithium-Ion Batteries: State of the Art and Perspectives. *ChemSusChem* **2015**, *8*, 2154−2175.
(7) Eshetu, G. G.; Grugeon, S.; Laruelle, S.; Boyanov, S.; Lecocq, A.; Bertrand, J. P.; Marlair, G. In-depth safety-focused analysis of solvents used in electrolytes for large scale lithium ion batteries. *Phys. Chem. Chem. Phys.* **2013**, *15*, 9145−9155.
(8) Hammami, A.; Raymond, N.; Armand, M. Lithium-ion batteries: runaway risk of forming toxic compounds. *Nature* **2003**, *424*, 635−636.
(9) James, S. L. Metal-organic frameworks. *Chem. Soc. Rev.* **2003**, *32*, 276.
(10) Furukawa, H.; Cordova, K. E.; O'Keeffe, M.; Yaghi, O. M. The chemistry and applications of metal-organic frameworks. *Science* **2013**, *341*, 1230444.
(11) Furukawa, H.; Ko, N.; Go, Y. B.; Aratani, N.; Choi, S. B.; Choi, E.; Yazaydin, A. O.; Snurr, R. Q.; O'Keeffe, M.; Kim, J.; Yaghi, O. M. Ultrahigh Porosity in Metal-Organic. *Science* **2010**, *329*, 424−428.
(12) Xia, W.; Mahmood, A.; Zou, R.; Xu, Q. Metal−organic frameworks and their derived nanostructures for electrochemical energy storage and conversion. *Energy Environ. Sci.* **2015**, *8*, 1837−1866.
(13) Zhao, X.; Xiao, B.; Fletcher, A. J.; Thomas, K. M.; Bradshaw, D.; Rosseinsky, M. J. Hysteretic adsorption and desorption of hydrogen by nanoporous metal-organic frameworks. *Science* **2004**, *306*, 1012−1015.
(14) Yaghi, O. M.; Li, G.; Li, H. Selective binding and removal of guests in a microporous metal−organic framework. *Nature* **1995**, *378*, 703−706.
(15) Hurd, J. A.; Vaidhyanathan, R.; Thangadurai, V.; Ratcliffe, C. I.; Moudrakovski, I. L.; Shimizu, G. K. Anhydrous proton conduction at 150 degrees C in a crystalline metal-organic framework. *Nat. Chem.* **2009**, *1*, 705−710.
(16) Chen, W. X.; Xu, H. R.; Zhuang, G. L.; Long, L. S.; Huang, R. B.; Zheng, L. S. Temperature-dependent conductivity of Emim+ (Emim+ = 1-ethyl-3-methyl imidazolium) confined in channels of a metal-organic framework. *Chem. Commun.* **2011**, *47*, 11933−11935.
(17) Fujie, K.; Yamada, T.; Ikeda, R.; Kitagawa, H. Introduction of an ionic liquid into the micropores of a metal-organic framework and its anomalous phase behavior. *Angew. Chem., Int. Ed.* **2014**, *53*, 11302−11305.
(18) Fujie, K.; Otsubo, K.; Ikeda, R.; Yamada, T.; Kitagawa, H. Low Temperature Ionic Conductor: Ionic Liquid Incorporated within a Metal−Organic Framework. *J. Name.* **2015**, *6*, 4306−4310.
(19) Fujie, K.; Ikeda, R.; Otsubo, K.; Yamada, T.; Kitagawa, H. Lithium Ion Diffusion in a Metal−Organic Framework Mediated by an Ionic Liquid. *Chem. Mater.* **2015**, *27*, 7355−7361.
(20) Park, S. S.; Tulchinsky, Y.; Dinca, M. Single-Ion Li+, Na+, and Mg2+ Solid Electrolytes Supported by a Mesoporous Anionic Cu-

Azolate Metal-Organic Framework. *J. Am. Chem. Soc.* **2017**, *139*, 13260−13263.
(21) Fischer, S.; Roeser, J.; Lin, T. C.; DeBlock, R. H.; Lau, J.; Dunn, B. S.; Hoffmann, F.; Froba, M.; Thomas, A.; Tolbert, S. H. A Metal−Organic Framework with Tetrahedral Aluminate Sites as a Single-Ion Li+ Solid Electrolyte. *Angew. Chem., Int. Ed.* **2018**, *57*, 16683−16687.
(22) Wiers, B. M.; Foo, M. L.; Balsara, N. P.; Long, J. R. A solid lithium electrolyte via addition of lithium isopropoxide to a metal-organic framework with open metal sites. *J. Am. Chem. Soc.* **2011**, *133*, 14522−14525.
(23) Qi, X. L.; Zhou, D. D.; Zhang, J.; Hu, S.; Haranczyk, M.; Wang, D. Y. Simultaneous Improvement of Mechanical and Fire-Safety Properties of Polymer Composites with Phosphonate-Loaded MOF Additives. *ACS Appl. Mater. Interfaces* **2019**, *11*, 20325−20332.
(24) Wang, Z.; Tan, R.; Wang, H.; Yang, L.; Hu, J.; Chen, H.; Pan, F. A Metal-Organic-Framework-Based Electrolyte with Nanowetted Interfaces for High-Energy-Density Solid-State Lithium Battery. *Adv. Mater.* **2018**, *30*, 1704436.
(25) Aubrey, M. L.; Ameloot, R.; Wiers, B. M.; Long, J. R. Metal−organic frameworks as solid magnesium electrolytes. *Energy Environ. Sci.* **2014**, *7*, 667.
(26) Zhao, C. Z.; Chen, P. Y.; Zhang, R.; Chen, X.; Li, B. Q.; Zhang, X. Q.; Cheng, X. B.; Zhang, Q. An ion redistributor for dendrite-free lithium metal anodes. *Sci. Adv.* **2018**, *4*, No. eaat3446.
(27) Wang, X.; Zhang, Y.; Zhang, X.; Liu, T.; Lin, Y. H.; Li, L.; Shen, Y.; Nan, C. W. Lithium-Salt-Rich PEO/Li0.3La0.557TiO3 Interpenetrating Composite Electrolyte with Three-Dimensional Ceramic Nano-Backbone for All-Solid-State Lithium-Ion Batteries. *ACS Appl. Mater. Interfaces* **2018**, *10*, 24791−24798.
(28) Heinze, M. T.; Zill, J. C.; Matysik, J.; Einicke, W. D.; Glaser, R.; Stark, A. Solid-ionic liquid interfaces: pore filling revisited. *Phys. Chem. Chem. Phys.* **2014**, *16*, 24359−24372.
(29) Hu, Z.; Zhang, S.; Dong, S.; Li, W.; Li, H.; Cui, G.; Chen, L. Poly(ethyl α-cyanoacrylate)-Based Artificial Solid Electrolyte Interphase Layer for Enhanced Interface Stability of Li Metal Anodes. *Chem. Mater.* **2017**, *29*, 4682−4689.
(30) Li, N. W.; Shi, Y.; Yin, Y. X.; Zeng, X. X.; Li, J. Y.; Li, C. J.; Wan, L. J.; Wen, R.; Guo, Y. G. A Flexible Solid Electrolyte Interphase Layer for Long-Life Lithium Metal Anodes. *Angew. Chem.* **2018**, *57*, 1521−1525.
(31) Mauger, A.; Armand, M.; Julien, C. M.; Zaghib, K. Challenges and issues facing lithium metal for solid-state rechargeable batteries. *J. Power Sources* **2017**, *353*, 333−342.

DOI: 10.1021/acsami.9b13712
ACS Appl. Mater. Interfaces 2019, 11, 46671−46677